IOPscience iopscience.iop.org

Home Search Collections Journals About Contact us My IOPscience

Non-monotonicity and divergent time scale in Axelrod model dynamics

This article has been downloaded from IOPscience. Please scroll down to see the full text article.

2007 EPL 78 18002

(http://iopscience.iop.org/0295-5075/78/1/18002)

View the table of contents for this issue, or go to the journal homepage for more

Download details:
IP Address: 128.197.40.148
The article was downloaded on 06/12/2010 at 17:57

Please note that terms and conditions apply.

A Letters Journal Exploring the Frontiers of Physics

April 2007

EPL, **78** (2007) 18002
doi: 10.1209/0295-5075/78/18002

www.epljournal.org

Non-monotonicity and divergent time scale in Axelrod model dynamics

F. Vazquez[a] and S. Redner

Center for BioDynamics, Center for Polymer Studies, and Department of Physics, Boston University - Boston, MA, 02215, USA

received 1 September 2006; accepted in final form 17 February 2007
published online 19 March 2007

PACS 89.65.-s – Social and economic systems
PACS 02.50.Ey – Stochastic processes
PACS 05.40.-a – Fluctuation phenomena, random processes, noise, and Brownian motion

Abstract – We study the evolution of the Axelrod model for cultural diversity, a prototypical non-equilibrium process that exhibits rich dynamics and a dynamic phase transition between diversity and an inactive state. We consider a simple version of the model in which each individual possesses two features that can assume q possibilities. Within a mean-field description in which each individual has just a few interaction partners, we find a phase transition at a critical value q_c between an active, diverse state for $q < q_c$ and a frozen state. For $q \lesssim q_c$, the density of active links is non-monotonic in time and the asymptotic approach to the steady state is controlled by a time scale that diverges as $(q - q_c)^{-1/2}$.

Copyright © EPLA, 2007

Introduction. – A basic feature of many societies is the tendency for cultural fragmentation, even though individuals may rationally try to reach agreement with acquaintances. A simple yet rich description for this dichotomy is provided by the Axelrod model [1]. Although inspired by social science, this model has many similarities with classical non-equilibrium processes of coarsening and dynamical transitions, such as the kinetic Ising model [2], the voter model [3], and birth-death processes [4].

In the Axelrod model, each individual carries a set of F characteristic features —for example, one's preferences for sports, for music, for food, etc.— that can assume q distinct values. In an update step, a pair of interacting agents i and j is selected. If the agents do not agree on any feature, there is no interaction. However, if the agents agree on at least one feature, they interact with a probability equal to the fraction of features that they share. When an interaction occurs, a previously unshared feature is selected at random and one agent copies this feature preference from its interaction partner. This tendency for consensus resembles the interaction of the voter model. However, restricting the interaction only to sufficiently compatible individuals leads to richer phenomenology. Similar interaction restrictions underlie the bounded confidence [5] and constrained voter-like models [6].

Depending on the parameters F and q, the Axelrod model undergoes a phase transition whose nature depends on the dimension of the system. For finite-size lattice systems in dimension d, a transition occurs between consensus (all agents in the same state) and frozen discordant state, where each interacting pair is incompatible [1,7–9]. In the mean-field limit, the transition is between an active steady state and a frozen discordant state. This rich behavior does not fall within the classical paradigms of coarsening in an interacting spin system [2] or diffusive approach to consensus in the voter model [3]. In this letter, we study a mean-field version of the Axelrod model in which each agent has a small and fixed number of interaction partners. We solve the master equations for the model dynamics and find a non-monotonic and extremely slow approach to the steady state, with a characteristic time scale that diverges as $q \to q_c$ (fig. 1).

The emergence of an anomalously long time scale in the Axelrod model is unexpected because the underlying master equations have rates that are of the order of one. Important examples where simple dynamics leads to wide time-scale separation and anomalous dynamics include, for example, the Lorenz strange attractor [10] and HIV [11]. In the former case, although the 3 coupled differential equations of the model represent a contracting map, the

[a] Current address: Instituto Mediterraneo de Estudios Avanzados (IMEDEA), CSIC-UIB Ed. Mateu Orfila - Campus UIB, E-07122 Palma de Mallorca, Spain.

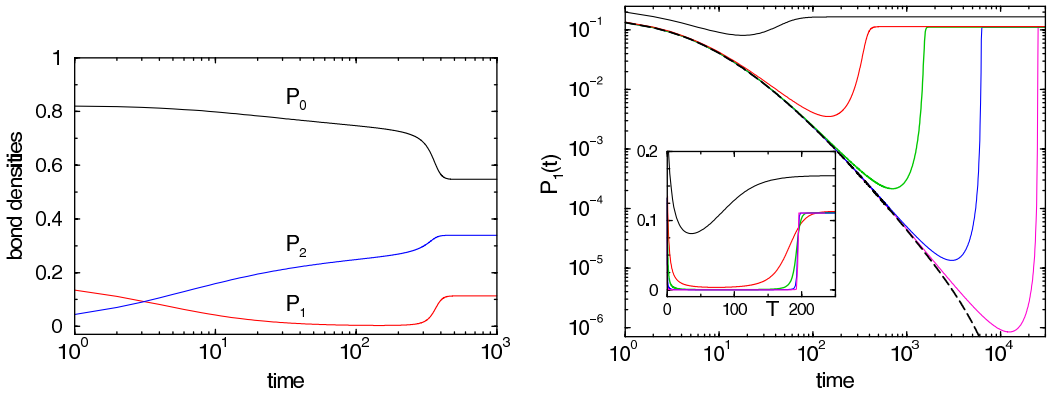

Fig. 1: (Left) Time dependence of bond densities P_0, P_1, and P_2 for $q = q_c - 4^{-1}$. Each agent has 4 neighbors. (Right) $P_1(t)$ for $q = q_c - 4^{-k}$, with $k = -1, 1, 3, 5$, and 7 (progressively lower minima). Each agent has 4 neighbors. The dashed curve shows how $P_1 \to 0$ for $q = q_c + 4^{-6}$. Inset: same data on a linear scale with $T = t(q - q_c)^{1/2}$.

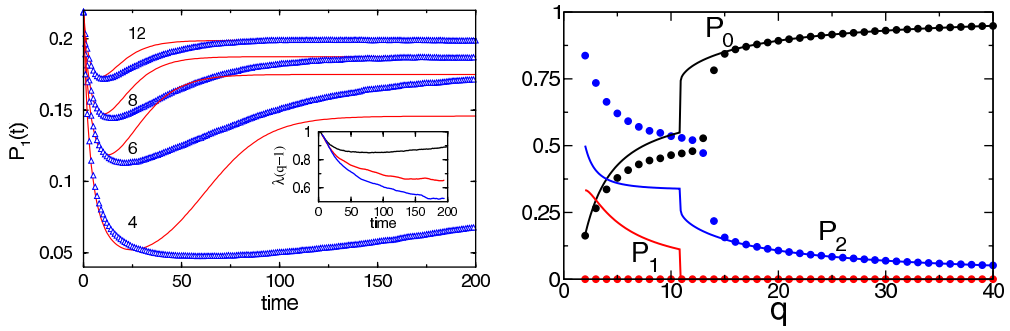

Fig. 2: (Left) Active bond density from the master equations (curves) and from simulations of 10^2 realizations ($\triangle$) on a degree-regular random graph with 10^4 nodes for various coordination numbers and $q = 8$ states per feature. Inset: time dependence of $\lambda(q-1)$ for $q = 8, 13$, and 20 (top to bottom). (Right) Final state bond densities P_i *vs.* q from simulations on a degree-regular random graph with 10^4 nodes and coordination number 4 (circles). A frozen final state is reached because the system is finite. Solid lines are the stationary master equation solutions with $P_1 > 0$ for $q < q_c$.

trajectories never reach a fixed point, but rather fall into a strange attractor. More germane to the present discussion is the case of HIV. After an individual contracts the disease, there is a normal immune response over a time scale of months, followed by a latency period that can last beyond 10 years, during which an individual's T-cell level slowly decreases with time. Finally, after the T-cell level falls below a threshold value, there is a final fatal phase that lasts 2–3 years. Our results for the Axelrod model provide some insights into how widely separated time scales arise in these types of complex dynamical systems. Although there is no direct connection between the Axelrod model and the examples of HIV dynamics and the Lorenz attractor, the study of systems with wide time-scale separation should ultimately provide a deeper general understanding.

Theory. – Following refs. [7,8], we describe the Axelrod model in a minimalist way by P_m, the density of bonds of type m. These are bonds between interaction partners that have m common features. This description is convenient for monitoring the activity of the system and has the advantage of being analytically tractable. We consider a mean-field system in which each agent can interact with a fixed but *finite* number of randomly selected agents. Agents can thus be viewed as being situated on the nodes of a degree-regular random graph. We verified that simulations of the Axelrod model on degree-regular random graphs qualitatively agree with our analytical predictions, and this agreement becomes progressively more accurate as the number of neighbors increases (fig. 2). Thus the master equations describe the Axelrod model on the degree-regular random graph over a substantial time range. However, the density of active bonds in a finite system must ultimately vanish due to fluctuations, even in the steady-state regime. This phenomenon cannot be captured by a master equation approach.

If interaction partners do not share any common features ($m = 0$) or if all features are common ($m = F$), then no interaction occurs across the intervening bond. Otherwise, two agents that are connected by an active bond of type m (with $0 < m < F$) interact with probability

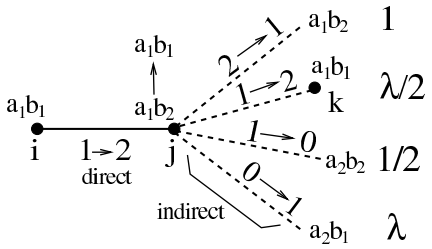

Fig. 3: State-changing bond updates when agent j changes state from $a_1b_2 \to a_1b_1$. The values at the right give the relative rates of each type of event.

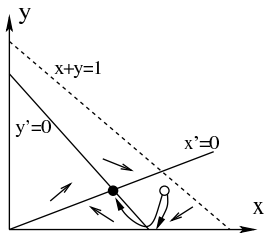

Fig. 4: Flow diagram in the x-y plane. The nullclines $x'=0$ and $y'=0$ meet at the steady-state fixed point (dot). The light arrows show the flow direction in the 4 regions of the composition triangle $x+y<1$. Shown schematically is a flow that starts at the uncorrelated initial state (circle) and ends on the axis $y=0$ for $q \gtrsim q_c$, and a flow that ends at the steady-state fixed point for $q \lesssim q_c$.

m/F, after which the bond necessarily becomes type $m+1$. In addition, when an agent changes a preference, the index of all indirect bonds attached to this agent may either increase or decrease (fig. 3). The competition between these direct and indirect interaction channels underlies the rich dynamics of the Axelrod model.

Because we obtain similar behavior for the density of active links, $P_a \equiv \sum_{k=1}^{F-1} P_k$, for all $F \geqslant 2$ in both simulations on degree-regular random graphs and in a master equation description that corresponds to the mean-field limit of the degree-regular random graph, we focus on the simplest non-trivial case of $F=2$, where there are three types of bonds: type 0 (no shared features) and type 2 (all features shared) are inert, while type 1 are active. As $q \to q_c$ from below, $P_a = P_1$ is non-monotonic, with an increasingly deep minimum (right panel in fig. 1), while for $q > q_c$, P_1 decays to zero exponentially with time. There is a discontinuous transition at q_c from a stationary phase where the steady-state density of active links P_1^s is greater than zero to a frozen phase where $P_1^s = 0$.

When fluctuations are neglected, the evolution of the bond densities P_m when a single agent changes its state is described by the master equations:

$$\frac{\mathrm{d}P_0}{\mathrm{d}t} = \frac{\eta}{\eta+1} P_1 \left[-\lambda P_0 + \frac{1}{2} P_1 \right], \tag{1}$$

$$\frac{\mathrm{d}P_1}{\mathrm{d}t} = -\frac{P_1}{\eta+1} + \frac{\eta}{\eta+1} P_1 \left[\lambda P_0 - \frac{1+\lambda}{2} P_1 + P_2 \right], \tag{2}$$

$$\frac{\mathrm{d}P_2}{\mathrm{d}t} = \frac{P_1}{\eta+1} + \frac{\eta}{\eta+1} P_1 \left[\frac{\lambda}{2} P_1 - P_2 \right], \tag{3}$$

where $\eta+1$ is the network coordination number. The first term on the right-hand sides of eqs. (2) and (3) accounts for the direct interaction between agents i and j that changes a bond of type 1 to type 2. For example, in the equation for $\frac{\mathrm{d}P_1}{\mathrm{d}t}$, a type-1 bond and the shared feature across this bond is chosen with probability $P_1/2$ in an update event. This update decrements the number of type-1 bonds by one in a time $\mathrm{d}t = \frac{1}{N}$, where N is the total number of sites in the system. Assembling these factors gives the term $-\frac{P_1}{\eta+1}$ in eq. (2).

The remaining terms in the master equations represent indirect interactions. For example, if agent j changes from (a_1, b_2) to (a_1, b_1) then the bond jk that joins to agent k in state (a_1, b_1) changes from type 1 to type 2 (fig. 3). The probability for this event is proportional to $P_1\lambda/2$: P_1 is the probability that the indirect bond is of type 1, the factor $1/2$ accounts for the fact that only the first feature of agents j and k can be shared, while λ is the conditional probability that i and k share one feature that is simultaneously not shared with j. If the distribution of preferences is uniform, then $\lambda = (q-1)^{-1}$. While λ generally depends on the densities P_m, our simulations give λ roughly constant and close to $(q-1)^{-1}$ (inset, left panel of fig. 2). We thus assume $\lambda = (q-1)^{-1}$ which renders the master equations soluble. Further evidence of the appropriateness of this assumption comes from the agreement between our simulations of the Axelrod model on random graphs with large coordination number and the master equation predictions (left panel, fig. 2).

Solution to the master equations. – We simplify the master equations by introducing the rescaled time $\mathrm{d}z = \frac{\eta}{\eta+1} P_1 \, \mathrm{d}t$, eliminating $P_2 = 1 - P_0 - P_1$, and defining $x = P_0$ and $y = P_1$, to obtain

$$\begin{aligned} x' &= -\lambda x + \frac{1}{2} y, \\ y' &= \left(1 - \frac{1}{\eta}\right) + (\lambda - 1) x - \left(\frac{3+\lambda}{2}\right) y, \end{aligned} \tag{4}$$

where the prime denotes derivative with respect to z. As shown in fig. 4, the nullclines $x'=0$ and $y'=0$ are given by $y = 2\lambda x$ and $\frac{2}{3+\lambda}[(1-\frac{1}{\eta}) + (\lambda-1)x]$, respectively, while there is an attracting fixed point (corresponding to a non-trivial steady state) at $(x^*, y^*) = \frac{\eta-1}{\eta(1+\lambda)^2}(1, 2\lambda)$. Analyzing the trajectories in this phase plane, we find the fundamental result that for $q > q_c$, the flow hits the axis $y=0$ (*i.e.*, $P_1^* = 0$) and the system is static, while for $q < q_c$, the steady-state fixed point with $P_1^* > 0$ is reached.

To determine the stationary solution of the master equations analytically, we set $\frac{\mathrm{d}P_i}{\mathrm{d}t} = 0$ in eqs. (1)-(3) and

solve, assuming $P_1 > 0$, to obtain

$$P_0^s = \frac{(\eta-1)}{\eta(1+\lambda)^2} = \frac{P_1^s}{2\lambda}, \qquad P_2^s = 1 - P_0^s - P_1^s. \tag{5}$$

Since $\lambda = \lambda(q)$ is the only free parameter in the master equations, the two distinct stationary solutions suggest that there is a transition at a critical value q_c. To locate the transition, it proves useful to relate P_1 and P_2 directly. Thus we divide eq. (2) by eq. (3) and eliminate P_0 via $P_0 = 1 - P_1 - P_2$ and obtain, after some algebra:

$$\frac{\mathrm{d}P_1}{\mathrm{d}P_2} = \frac{-1+\eta\lambda-\frac{1}{2}\eta(1+3\lambda)P_1+\eta(1-\lambda)P_2}{1+\frac{1}{2}\eta\lambda P_1-\eta P_2}, \tag{6}$$

whose solution has the form $P_1 = \alpha + \beta P_2 - \sqrt{\gamma+\delta P_2}$, where we determine the coefficients α, β, γ and δ by matching terms of the same order in eq. (6) and in this trial form. This procedure gives the solution except for one constant that is specified by the initial conditions. If the features for each agent are chosen uniformly from the integers $[0, q-1]$, the distribution of initial bond densities is binomial, $P_m(t=0) = \frac{2!}{m!(2-m)!}(1/q)^m(1-1/q)^{2-m}$. Matching this initial condition to the trial solution gives

$$P_1(P_2) = \frac{2\lambda}{1+\lambda} + \frac{2}{\eta} - 2P_2 - \frac{2}{\eta}\frac{\sqrt{\eta\lambda^2+(1+\lambda)^2(1-\eta P_2)}}{(1+\lambda)}. \tag{7}$$

As a function of P_2, P_1 has a minimum $P_1^{\min}(q)$ that monotonically decreases as q increases and becomes negative for q larger than a critical value q_c. The phase transition between the active and the frozen state corresponds to the value of q where P_1 first reaches zero. To find q_c, we calculate $P_1^{\min}$ as a function of $\lambda(q)$ from eq. (7) and find the value of q at which $P_1^{\min}$ becomes zero. This leads to

$$P_1^{\min} = \frac{4\eta\lambda-(1+\lambda)^2}{2\eta(1+\lambda)^2} \equiv \frac{S(\lambda,\eta)}{2\eta(1+\lambda)^2},$$

from which the critical point is $q_c = 2\eta + 2\sqrt{\eta(\eta-1)}$, while $P_1^{\min} \propto S \propto (q_c - q)$ for $q < q_c$.

We now determine the steady-state bond densities in the frozen state. From eq. (7), we compute the stationary value P_2^s at the point where P_1 first reaches zero. The smallest root of this equation then gives

$$P_2^s = \frac{1+\lambda+2\eta\lambda-\sqrt{(1+\lambda)^2-4\eta\lambda}}{2\eta(1+\lambda)},$$
$$P_0^s = 1 - P_2^s.$$

The most interesting behavior is the time dependence of the density of active bonds, $P_1(t)$. We solve for $P_1(t)$ by first inverting eq. (7) to express P_2 in terms of P_1:

$$P_2(P_1) = \frac{1+\lambda(1+2\eta)}{2\eta(1+\lambda)} - \frac{P_1}{2} - \frac{\sqrt{2\eta(1+\lambda)^2P_1-S}}{2\eta(1+\lambda)},$$

and then writing $P_0 = 1 - P_1 - P_2(P_1)$ also in terms of P_1, and finally substituting these results into the master equation (2) for P_1. After some algebra, we obtain

$$\frac{\mathrm{d}P_1}{\mathrm{d}\tau} = SP_1 - (1-\lambda)\sqrt{2\eta(1+\lambda)^2P_1 - S}\,P_1 - 2\eta(1+\lambda)^2P_1^2, \tag{8}$$

with rescaled time variable $\tau = \frac{t}{2(\eta+1)(1+\lambda)}$. This master equation can be simplified by substituting the quantity $\Delta \equiv 2\eta(1+\lambda)^2P_1 - S$, which measures the deviation of P_1 from its minimum value, in eq. (8). We obtain

$$\frac{\mathrm{d}\Delta}{\mathrm{d}\tau} = -\sqrt{\Delta}(S+\Delta)(1-\lambda+\sqrt{\Delta}). \tag{9}$$

Integrating by a partial fraction expansion gives

$$\tau = \frac{1}{4\lambda(\eta-1)}\left[\ln\left(\frac{S+\Delta}{\eta\lambda(1-\lambda)^2}\right) - 2\ln\left(1 \pm \frac{\sqrt{\Delta}}{1-\lambda}\right) + \frac{1-\lambda}{\sqrt{-S}}\ln\left(\frac{(\sqrt{-S}-1-\lambda)(\sqrt{-S}\pm\sqrt{\Delta})}{(\sqrt{-S}+1+\lambda)(\sqrt{-S}\mp\sqrt{\Delta})}\right)\right]. \tag{10}$$

For $q > q_c$, only the upper sign is needed. For $q < q_c$, the upper sign applies for $t < t^{\min}$ and the lower sign applies for $t > t^{\min}$; here $t^{\min}$ is the time at which $P_1(t)$ reaches its minimum value. Substituting back t and P_1 in eq. (10) gives the formal exact solution of eq. (8).

For $q < q_c$, we determine $P_1(t)$ near its minimum by taking the $\Delta \to 0$ limit of eq. (9) to give $\frac{\mathrm{d}\Delta}{\mathrm{d}t} \approx -aS\sqrt{\Delta}$, with $a = \frac{(1-\lambda)}{2(\eta+1)(1+\lambda)} > 0$. For $S > 0$, this lowest-order approximation leads to a quadratic form for P_1 around its minimum:

$$P_1(t) - P_1^{\min} \propto \Delta \approx \frac{a^2S^2}{8\eta(1+\lambda)^2}(t-t_{\min})^2. \tag{11}$$

When $q \to q_c$, the factor S in eq. (9) may be neglected as long as $\Delta > S$, and this leads to Δ decaying as t^{-2} before the minimum in P_1 is reached (dashed line on the right of fig. 1).

For q less than but close to the critical value q_c, P_1 has a peculiar time dependence as shown in the right panel of fig. 1. The density of active bonds P_1 quickly decreases with time and remains close to zero over a wide range when q is close to q_c. However, P_1 ultimately increases and reaches a non-zero asymptotic value for $q < q_c$. The quasi-stationary regime where P_1 remains small is defined by: i) a short time scale that characterizes the initial decay of $P_1(t)$, and ii) a much longer time scale t_{asymp}, where P_1 rapidly increases and then saturates at its steady-state value.

We can give a partial explanation for the time dependence of P_1. For $q > q_c$, there are initially small enclaves of interacting agents in a frozen discordant background. Once these enclaves reach local consensus, they are

incompatible with the background and the system freezes. For $q \lesssim q_c$ there is less diversity and sufficient active interfaces are present to allow partial coarsening into domains whose occupants are either compatible (that is, interacting) or identical. Within a domain of interacting agents, the active interface can ultimately migrate to the domain boundary and facilitate merging with other domains; this process corresponds to the sharp drop in P_0 seen in fig. 1 [12]. While this picture is presented in the context of a lattice system, remarkably it still seems to apply for in a mean-field description of degree-regular random graphs.

Both $t_{\min}$, as well as the end time of the quasi-stationary period t_{asymp}, increase continuously and diverge as q approaches q_c from below. To find these divergences, we expand $t_{\min}$ and t_{asymp} in powers of S. From eq. (10), the first two terms in the expansion of $t_{\min}$, as $S \to 0$, are $t_{\min} \equiv t(P_1^{\min}) \approx \text{const}/\sqrt{S} + \mathcal{O}(\ln S)$. Thus $t_{\min} \sim (q_c - q)^{-1/2}$ as $q \to q_c$. Similarly, we estimate t_{asymp} as the time at which P_1 reaches one-half of its steady-state value. Using eqs. (5) and (10), we find $t_{\text{asymp}} \equiv t(P_1^s/2) \sim 1/\sqrt{S} \sim (q_c - q)^{-1/2}$ as $q \to q_c$.

For $q > q_c$, the system evolves to a frozen state with $P_1 \to 0$. To lowest order eq. (8) becomes $\frac{\mathrm{d}P_1}{\mathrm{d}t} = -\frac{P_1}{\mathcal{T}}$, with $\mathcal{T} = \frac{2(\eta+1)(1+\lambda)}{-S+(1-\lambda)\sqrt{-S}}$ ($\mathcal{T} > 0$ since $S < 0$ for $q > q_c$). Consequently, P_1 decays exponentially in time as $t \to \infty$. As q approaches q_c, S asymptotically vanishes as $(q_c - q)$ and the leading behavior is $\mathcal{T} \sim (q - q_c)^{-1/2}$. Thus again there is an extremely slow approach to the asymptotic state as q approaches q_c.

Summary. – In summary, two striking features of the Axelrod model in the mean-field limit have an analytic explanation: the non-monotonic time dependence of the density of active links, and the anomalously long dynamical time scale. For $q < q_c$, an active steady state is reached in a time that diverges as $(q_c - q)^{-1/2}$ when $q \to q_c$ from below. For $q > q_c$, the final state is static and the time scale to reach this state also diverges as $(q_c - q)^{-1/2}$ as $q \to q_c$ from above.

* * *

We thank A. Vespignani for helpful comments on the manuscript and gratefully acknowledge financial support from the US National Science Foundation grant DMR0535503.

REFERENCES

[1] Axelrod R., *J. Conflict Res.*, **41** (1977) 203; Axtell R., Axelrod R., Epstein J. and Cohen M. D., *Comput. Math. Organiz. Theory*, **1** (1996) 123.

[2] Glauber R. J., *J. Math. Phys.*, **4** (1963) 294; Gunton J. D., San Miguel M. and Sahni P. S., *Phase Transitions and Critical Phenomena*, edited by Domb C. and Lebowitz J. L., Vol. **8** (Academic, New York) 1983; Bray A. J., *Adv. Phys.*, **43** (1994) 357.

[3] Liggett T. M., *Interacting Particle Systems* (Springer-Verlag, New York) 1985; Krapivsky P. L., *Phys. Rev. A*, **45** (1992) 1067.

[4] See *e.g.*, Marro J. and Dickman R., *Nonequilibrium Phase Transitions in Lattice Models* (Cambridge University Press, Cambridge) 1999; Hinrichsen H., *Adv. Phys.*, **49** (2000) 815.

[5] Weisbuch G., Deffuant G., Amblard F. and Nadal J. P., *Complexity*, **7** (2002) 55; Ben-Naim E., Krapivsky P. L. and Redner S., *Physica D*, **183** (2003) 190.

[6] Vazquez F. and Redner S., *J. Phys. A*, **37** (2004) 8479.

[7] Castellano C., Marsili M. and Vespignani A., *Phys. Rev. Lett.*, **85** (2000) 3536.

[8] Vilone D., Vespignani A. and Castellano C., *Eur. Phys. J. B*, **30** (2002) 399.

[9] Klemm K., Eguiluz V. M., Toral R. and San Miguel M., *Phys. Rev. E*, **67** (2003) 026120; Klemm K., Eguiluz V. M., Toral R. and San Miguel M., cond-mat/0205188; cond-mat/0210173; physics/0507201.

[10] Lorenz E. N., *J. Atmos. Sci.*, **20** (1963) 130.

[11] See, *e.g.*, Perelson A. S. and Nelson P. W., *SIAM Rev.*, **41** (1999) 3.

[12] For a java applet to visualize these phenomena, see `http://www.imedea.uib.es/physdept/research_topics/socio/culture.html`.